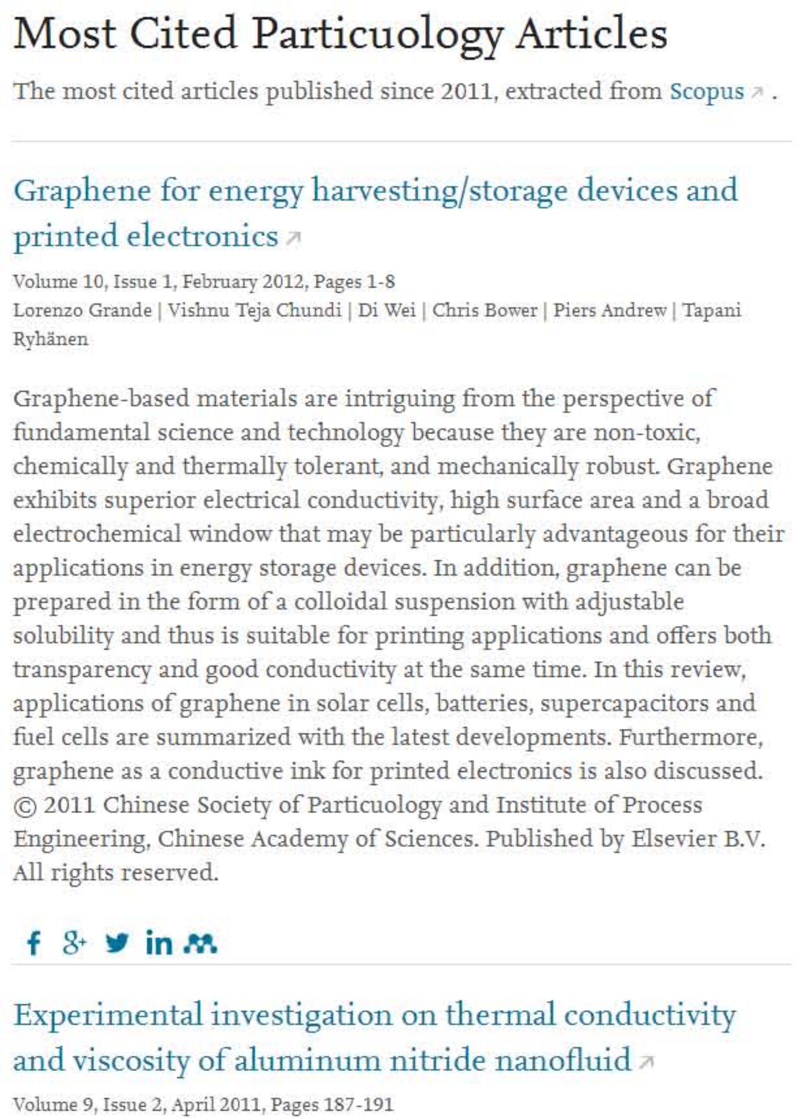

Most Cited Particuology Articles

The most cited articles published since 2011, extracted from Scopus.

Graphene for energy harvesting/storage devices and printed electronics

Volume 10, Issue 1, February 2012, Pages 1-8

Lorenzo Grande | Vishnu Teja Chundi | Di Wei | Chris Bower | Piers Andrew | Tapani Ryhänen

Graphene-based materials are intriguing from the perspective of fundamental science and technology because they are non-toxic, chemically and thermally tolerant, and mechanically robust. Graphene exhibits superior electrical conductivity, high surface area and a broad electrochemical window that may be particularly advantageous for their applications in energy storage devices. In addition, graphene can be prepared in the form of a colloidal suspension with adjustable solubility and thus is suitable for printing applications and offers both transparency and good conductivity at the same time. In this review, applications of graphene in solar cells, batteries, supercapacitors and fuel cells are summarized with the latest developments. Furthermore, graphene as a conductive ink for printed electronics is also discussed.

© 2011 Chinese Society of Particuology and Institute of Process Engineering, Chinese Academy of Sciences. Published by Elsevier B.V. All rights reserved.

Experimental investigation on thermal conductivity and viscosity of aluminum nitride nanofluid

Volume 9, Issue 2, April 2011, Pages 187-191

Wei Yu | Huaqing Xie | Yang Li | Lifei Chen

Aluminum nitride nanoparticles (AlNs) have been found to be a good additive for enhancing the thermal conductivity of traditional heat exchange fluids. At a volume fraction of 0.1, the thermal conductivity enhancement ratios are 38.71% and 40.2%, respectively, for ethylene glycol and propylene glycol as the base fluids. Temperature does not have much influence on the enhanced thermal conductivity ratios of the nanofluids, though a volume fraction of 5.0% appears to signify a critical concentration for rheology: for <5.0 vol% for Newtonian behavior, and for >5.0 vol% for obvious shear-shinning behavior, for both ethylene glycol and propylene glycol. © 2011 Chinese Society of Particuology and Institute of Process Engineering, Chinese Academy of Sciences.

Chemical composition of PM2.5 during winter in Tianjin, China

Volume 9, Issue 3, June 2011, Pages 215-221
Jinxia Gu | Zhipeng Bai | Weifang Li | Liping Wu | Aixia Liu | Haiyan Dong | Yiyang Xie

PM2.5 samples for 24 h were collected during winter in Tianjin, China. The ambient mass concentration and chemical composition of the PM 2.5 were determined. Ionic species were analyzed by ion chromatography, while carbonaceous species were determined with the IMPROVE thermal optical reflectance (TOR) method, and inorganic elements were measured by inductively coupled plasma-atomic emission spectrometer. The daily PM 2.5 mass concentrations ranged from 48.2 to 319.2 µg/m3 with an arithmetic average of 144.6 µg/m3. The elevated PM 2.5 in winter was mostly attributed to combustion sources such as vehicle exhaust, heating, cooking and industrial emissions, low wind speeds and high relative humidity (RH), which were favorable for pollutant accumulation and formation of secondary

pollutants. By chemical mass balance, it was estimated that about 89.1% of the PM2.5 mass concentrations were explained by carbonaceous species, secondary particles, crustal matters, sea salt and trace elements. Organic material was the largest contributor, accounting for about 32.7% of the total PM2.5 mass concentrations. SO_4^{2-}, NO_3^-, Cl^- and NH_4^+ were four major ions, accounting for 16.6%, 11.5%, 4.7% and 6.0%, respectively, of the total mass of PM2.5.
© 2011 Chinese Society of Particuology and Institute of Process Engineering, Chinese Academy of Sciences. Published by Elsevier B.V. All rights reserved.

PM2.5 in China: Measurements, sources, visibility and health effects, and mitigation ↗

Volume 13, Issue 1, January 2014, Pages 1-26
David Y H Pui | Sheng Chieh Chen | Zhili Zuo

Concern over the health effects of fine particles in the ambient environment led the U.S. Environmental Protection Agency to develop the first standard for PM2.5 (particulate matter less than 2.5 μm) in 1997. The Particle Technology Laboratory at the University of Minnesota has helped to establish the PM2.5 standard by developing many instruments and samplers to perform atmospheric measurements. In this paper, we review various aspects of PM2.5, including its measurement, source apportionment, visibility and health effects, and mitigation. We focus on PM2.5 studies in China and where appropriate, compare them with those obtained in the U.S. Based on accurate PM2.5 sampling, chemical analysis, and source apportionment models, the major PM2.5 sources in China have been identified to be coal combustion, motor vehicle emissions, and industrial sources. Atmospheric visibility has been found to correlate well with PM 2.5 concentration. Sulfate, ammonium, and nitrate carried by PM 2.5, commonly found in coal burning and vehicle emissions, are the dominant contributors to regional haze in China. Short-term exposure

to PM 2.5 is strongly associated with the increased risk of morbidity and mortality from cardiovascular and respiratory diseases in China. The strategy for PM2.5 mitigation must be based on reducing the pollutants from the two primary sources of coal-fired power plants and vehicle emissions. Although conventional Particulate Emission Control Devices (PECD) such as electrostatic precipitators in Chinese coal-fired power plants are generally effective for large particles, most of them may not have high collection efficiency of PM2.5. Baghouse filtration is gradually incorporated into the PECD to increase the PM2.5 collection efficiency. By adopting stringent vehicle emissions standard such as Euro 5 and 6, the emissions from vehicles can be gradually reduced over the years. An integrative approach, from collaboration among academia, government, and industries, can effectively manage and mitigate the PM2.5 pollution in China. © 2013 Chinese Society of Particuology and Institute of Process Engineering, Chinese Academy of Sciences.

Influence of rolling friction on single spout fluidized bed simulation ↗

Volume 10, Issue 5, October 2012, Pages 582-591

Christoph Goniva | Christoph Kloss | Niels G. Deen | Johannes A M Kuipers | Stefan Pirker

In this paper we study the effect of rolling friction on the dynamics in a single spout fluidized bed using Discrete Element Method (DEM) coupled to Computational Fluid Dynamics (CFD). In a first step we neglect rolling friction and show that the results delivered by the open source CFD-DEM framework applied in this study agree with previous simulations documented in literature. In a second step we include a rolling friction sub-model in order to investigate the effect of particle non-sphericity. The influence of particle-particle as well as particle-wall rolling friction on the flow in single spout fluidized bed is studied separately. Adequate rolling friction model parameters are obtained

using first principle DEM simulations and data from literature. Finally, we demonstrate the importance of correct modelling of rolling friction for coupled CFD-DEM simulations of spout fluidized beds. We show that simulation results can be improved significantly when applying a rolling friction model, and that experimental data from literature obtained with Positron Emission Particle Tracking (PEPT) technique can be satisfactorily reproduced. © 2012 Chinese Society of Particuology and Institute of Process Engineering, Chinese Academy of Sciences.

Mixing of powders and granular materials by mechanical means - A perspective

Volume 10, Issue 4, August 2012, Pages 397-427
John Bridgwater

When engineers and scientists encounter the mixing of powders, they enter a subject where it is often difficult to find bearings. This perspective seeks to address this need by setting out the state of practice. It then considers the growing momentum in the area following advances in computation and in measurement that became significant in the 1990s. The mixing of powders and granular materials is of central importance for the quality and performance of a wide range of products. However, process design and operation are very difficult, being largely based on judgement rather than science. There are not even tabulated data to tell how the quality of mixtures depends on mixer selection. Design depends on experience and insight, not science. There are no sound scale-up laws for a given equipment type, largely because particle size needs to be included in any dimensional analysis. Design is not possible by applying physical principles. There is no reliable equation to describe the flow of single component powders, let alone multi-component mixtures. In most cases, measurement has been difficult because the materials are optically opaque. Work in the research literature has been questionable because the results obtained

for mixture sampling are affected by sample size. Recently, modern experimental techniques and modelling work have provided a good deal of information on the behaviour of many of the pieces of equipment, though these have been small in size and often confined to materials of a single size. However, the studies have enhanced knowledge of physical behaviour. For example, for a wide range of equipment when operating at lower velocities, mixing is determined by the number of revolutions of the mixer, not the time. Observations of flow structure have led to a few specific models that should scale with equipment size. Measurement techniques are slowly becoming more effective in giving internal flow patterns and in measuring powder composition. For cohesionless and cohesive materials, DEM (Discrete Element Method) codes are now commonly being used to describe flow patterns on the scale of 10,000-250,000 particles with a few workers using an order of magnitude more particles. A strategy that embraces the effects of particle size, equipment size and internal geometry, is advocated for the future. The aim would be to elucidate engineering principles of general utility. As part of the overall approach, findings must be backed by experiment. For cohesive materials, there is scope to develop methods coming from population balance modelling. There is also scope to develop an understanding by subjecting well-defined cohesive materials to clear patterns of strain. It may now be possible to use the methods of (say) digital photography to obtain data which can be fed into a method of mixture characterisation that is free of the problems of sample size. Together with an understanding of the relationship between observation at a surface and the average of a flow as a whole, such a method would, if successful, be of immense utility. At the very least, performance charts for industrial equipment would finally become available. The next stage of development is to build on the emerging knowledge and methods so that the basics for design can be laid down. Then design can become predictable with operation giving effective control of performance. © 2012 Chinese Society of Particuology and Institute of Process Engineering, Chinese Academy of Sciences. Published by Elsevier B.V. All rights reserved.

Controllable preparation of particles with microfluidics

Volume 9, Issue 6, December 2011, Pages 545-558

Guangsheng Luo | Le Du | Yujun Wang | Yangcheng Lu | Jianhong Xu

This paper reviews recent development and achievements in controllable preparation of nanoparticles, micron spherical and non-spherical particles, using microfluidics. A variety of synthesis strategies are presented and compared, including single-phase and multiphase microflows. The main structures of microfluidic devices and the fundamental principles of microflows for particle preparation are summarized and identified. The controllability of particle size, size distribution, crystal structure, morphology, physical and chemical properties, is examined in terms of the special features of microfluidic reactors. An outlook on opinions and predictions concerning the future development of powder technology with microfluidics is specially provided. © 2011 Chinese Society of Particuology and Institute of Process Engineering, Chinese Academy of Sciences.

Effect of particle shape and size on flow properties of lactose powders

Volume 10, Issue 2, April 2012, Pages 203-208

Xiaowei Fu | Deborah Huck | Lisa Makein | Brian Armstrong | Ulf Willen | Tim Freeman

The shape and size of particles are understood to affect the bulk behaviour of powders, though there are but few studies that present quantitative information on the relationship between particle shape and the flow properties of powder. This is due in part to the lack of techniques for rapidly determining both particle shape and the range of flow characteristics that describe the response of powders to the stress

and shear experienced during their processing. This study presents data that quantifies the influence of particle shape/size of three different lactose powders on their respective flow and bulk characteristics. Two of the samples differ in size but have similar shapes; the third sample is more spherical but similar in size to one of the other two samples. The results demonstrate that in addition to particle size, particle shape significantly affect the flow characteristics of a powder over a wide range of stress conditions. © 2012 Chinese Society of Particuology and Institute of Process Engineering, Chinese Academy of Sciences. Published by Elsevier B.V. All rights reserved.

Evolution of planetary boundary layer under different weather conditions, and its impact on aerosol concentrations ↗

Volume 11, Issue 1, February 2013, Pages 34-40

Jiannong Quan | Yang Gao | Qiang Zhang | Xuexi Tie | Junji Cao | Suqin Han | Junwang Meng | Pengfei Chen | Delong Zhao

A field experiment was conducted in Tianjin, China from September 9-30, 2010, focused on the evolution of Planetary Boundary Layer (PBL) and its impact on surface air pollutants. The experiment used three remote sensing instruments, wind profile radar (WPR), microwave radiometer (MWR) and micro-pulse lidar (MPL), to detect the vertical profiles of winds, temperature, and aerosol backscattering coefficient and to measure the vertical profiles of surface pollutants (aerosol, CO, SO2, NOx), and also collected sonic anemometers data from a 255-m meteorological tower. Based on these measurements, the evolution of the PBL was estimated. The averaged PBL height was about 1000-1300 m during noon/afternoon-time, and 200-300 m during night-time. The PBL height and the aerosol concentrations were anti-correlated during clear and haze conditions. The averaged maximum PBL heights were 1.08 and 1.70 km while the averaged aerosol concentrations were 52 and

17 μg/m 3 under haze and clear sky conditions, respectively. The influence of aerosols and clouds on solar radiation was observed based on sonic anemometers data collected from the 255-m meteorological tower. The heat flux was found significantly decreased by haze (heavy pollution) or cloud, which tended to depress the development of PBL, while the repressed structure of PBL further weakened the diffusion of pollutants, leading to heavy pollution. This possible positive feedback cycle (more aerosols → lower PBL height → more aerosols) would induce an acceleration process for heavy ground pollution in megacities. © 2012 2012 Chinese Society of Particuology and Institute of Process Engineering, Chinese Academy of Sciences. Published by Elsevier B.V. All rights reserved.

Hydrothermal synthesis and physicochemical characterization of CuO/ZnO/Al2O3 nanopowder. Part I: Effect of crystallization time ↗

Volume 10, Issue 6, December 2012, Pages 729-736

Saeed Saedy | Mohammad Haghighi | Mahsa Amirkhosrow

A hydrothermal method was successfully used for synthesis of CuO/ZnO/Al2O3 (CZA) nanopowder with atomic ratio of 6:3:1. The effect of crystallization time (3, 6, 9, and 12 h) on physicochemical properties of nanopowder was investigated. Nanopowders were characterized using XRD, FESEM, EDX, FTIR, TG, and BET techniques. The XRD patterns confirmed metal oxides formation and their good crystallinity with average crystallite size of 20 nm as obtained by the Scherrer equation. Relative crystallinity was shown to increase with increasing crystallization time. In agreement with XRD results, FESEM images also illustrated nanosized particles. EDX mapping indicated homogenous dispersion of elements. BET specific surface area analysis showed acceptable surface area for CZA nanopowder. FTIR spectroscopy confirmed metal oxides formation during hydrothermal and calcination

processing. TG results illustrated high thermal stability of the synthesized nanopowders. TG-DTG and FTIR analyses were used to propose a reaction mechanism for nanopowder formation during processing. Physicochemical characterization showed optimal crystallization time to be 6 h. © 2012 Chinese Society of Particuology and Institute of Process Engineering, Chinese Academy of Sciences.

CFD-DEM study of effect of bed thickness for bubbling fluidized beds ↗

Volume 10, Issue 5, October 2012, Pages 532-541

Tingwen Li | Pradeep Gopalakrishnan | Rahul Garg | Mehrdad Shahnam

The effect of bed thickness in rectangular fluidized beds is investigated through the CFD-DEM simulations of small-scale systems. Numerical results are compared for bubbling fluidized beds of various bed thicknesses with respect to particle packing, bed expansion, bubble behavior, solids velocities, and particle kinetic energy. Good two-dimensional (2D) flow behavior is observed in the bed having a thickness of up to 20 particle diameters. However, a strong three-dimensional (3D) flow behavior is observed in beds with a thickness of 40 particle diameters, indicating the transition from 2D flow to 3D flow within the range of 20-40 particle diameters. Comparison of velocity profiles near the walls and at the center of the bed shows significant impact of the front and back walls on the flow hydrodynamics of pseudo-2D fluidized beds. Hence, for quantitative comparison with experiments in pseudo-2D columns, the effect of walls has to be accounted for in numerical simulations. © 2012 Chinese Society of Particuology and Institute of Process Engineering, Chinese Academy of Sciences.

Quasi-real-time simulation of rotating drum using discrete element method with parallel GPU computing

Volume 9, Issue 4, August 2011, Pages 446-450

Ji Xu | Huabiao Qi | Xiaojian Fang | Liqiang Lu | Wei Ge | Xiaowei Wang | Ming Xu | Feiguo Chen | Xianfeng He | Jinghai Li

Real-time simulation of industrial equipment is a huge challenge nowadays. The high performance and fine-grained parallel computing provided by graphics processing units (GPUs) bring us closer to our goals. In this article, an industrial-scale rotating drum is simulated using simplified discrete element method (DEM) without consideration of the tangential components of contact force and particle rotation. A single GPU is used first to simulate a small model system with about 8000 particles in real-time, and the simulation is then scaled up to industrial scale using more than 200 GPUs in a 1D domain-decomposition parallelization mode. The overall speed is about 1/11 of the real-time. Optimization of the communication part of the parallel GPU codes can speed up the simulation further, indicating that such real-time simulations have not only methodological but also industrial implications in the near future. © 2011 Published by Elsevier B.V. on behalf of Chinese Society of Particuology and Institute ofProcess Engineering, Chinese Academy of Sciences.

Flexible supercapacitors

Volume 11, Issue 4, August 2013, Pages 371-377

Shan Shi | Chengjun Xu | Cheng Yang | Jia Li | Hongda Du | Baohua Li | Feiyu Kang

Flexible supercapacitors show a great potential for applications in wearable, miniaturized, portable, large-scale transparent and flexible consumer electronics due to their significant, inherent advantages, such as being flexible, lightweight, low cost and environmentally friendly in

comparison with the current energy storage devices. In this report, recent progress on flexible supercapacitors, flexible electrodes and electrolytes is reviewed. In addition, the future challenges and opportunities are discussed. © 2013 Chinese Society of Particuology and Institute of Process Engineering, Chinese Academy of Sciences.

Yarn spun from carbon nanotube forests: Production, structure, properties and applications ↗

Volume 11, Issue 4, August 2013, Pages 378-393

Menghe Miao

The discovery of drawable carbon nanotube forests opened up the possibility of constructing a wide range of pure carbon nanotube macrostructures and sparked interests in developing applications from these structures, especially pure carbon nanotube yarns. This review examines the various facets of the drawable carbon nanotube forests, synthesis and drawability, and their resulting yarns, structure, production, properties and applications. The structure, formation and properties of carbon nanotube yarns are compared with those of conventional textile yarns in order to obtain a better understanding of the science, structural mechanics and processing technology involved in carbon nanotube yarns. © 2013 Chinese Society of Particuology and Institute of Process Engineering, Chinese Academy of Sciences.

Pressure drop of TiO2 nanofluid in circular pipes ↗

Volume 9, Issue 5, October 2011, Pages 486-491

Tun Ping Teng | Yi Hsuan Hung | Ching Song Jwo | Chien Chih Chen | Lung Yue Jeng

This paper discusses the pressure drop in circular pipes of TiO 2/water nanofluid for both laminar and turbulent flows at different temperatures and TiO2 weight fractions. This study shows that TiO2/water nanofluid causes enhancement, but temperature rise reduces pressure drop. The proportional increase in pressure drop for turbulent flow is lower than that for laminar flow. The traditional equation for pressure drop fails to accurately estimate the pressure drop for laminar and turbulent flows. Accordingly, this study developed new empirical equations for the friction factor for both laminar and turbulent flows, and the maximum deviations between calculated and experimental results were reduced to within the ranges of -6.17% to 3.55% and -3.08% to 3.81%, respectively, that is, for TiO2/water nanofluid, the correlations apply better to turbulent than to laminar flow. © 2011 Chinese Society of Particuology and Institute of Process Engineering, Chinese Academy of Sciences.

Technical challenges in tackling regulatory concerns for urban atmospheric nanoparticles ↗

Volume 9, Issue 6, December 2011, Pages 566-571

Prashant Kumar | Alan Robins | Sotiris Vardoulakis | Paul Quincey

Recent Euro 5 and Euro 6 vehicle emission standards are the first ever initiative to control particles on a number basis at the source. Related standards are also desirable for ambient nanoparticles (taken in this article to be those below 300 nm) to protect against possible adverse effects on public health and the environment. However, there are a number of technical challenges that need to be tackled before developing a regulatory framework for atmospheric nanoparticles. Some of the challenges derive from a lack of standardisation of the key measurement parameters, including sampling, necessary for robust evaluation of particle number concentrations, especially in the context of insufficient knowledge of the physicochemical characteristics of emerging sources (i.e. bio-fuel derived and manufactured nanoparticles). Ideally, ambient concentrations of primary particles

could be linked to primary particle emissions by use of nanoparticle dispersion models, and secondary nanoparticles using photochemical modeling tools. The limitations in these areas are discussed. Although there is inadequate information on the exact biological mechanism through which these particles cause harm, it is argued that this should not in itself delay the introduction of regulation. This article reviews the missing links between the existing knowledge of nanoparticle number concentrations and the advances required to tackle the technical challenges implied in developing regulations. © 2011 Chinese Society of Particuology and Institute of Process Engineering, Chinese Academy of Sciences.

Synthesis of iron oxide nanoparticles via sonochemical method and their characterization ↗

Volume 9, Issue 1, February 2011, Pages 95-99

Amir Hassanjani-Roshan | Mohammad Reza Vaezi | Ali Shokuhfar | Zohreh Rajabali

Preparation of iron oxide (α-Fe2O3) nanoparticles was carried out via a sonochemical process. The process parameters such as temperature, sonication time and power of ultrasonication play important roles in the size and morphology of the final products. The iron oxide nanoparticles were characterized by transmission electron microscopy, X-ray powder diffraction, and thermogravimetric and differential thermal analyses. From transmission electron microscopy observations, the size of the iron oxide nanoparticles is estimated to be significantly smaller than 19 nm. X-ray diffraction data of the powder after annealing provide direct evidence that the iron oxide was formed during the sonochemical process. © 2010 Chinese Society of Particuology and Institute of Process Engineering, Chinese Academy of Sciences.

Non-uniform distribution of gas-solid flow through six parallel cyclones in a CFB system: An experimental study

Volume 10, Issue 2, April 2012, Pages 170-175

Xinglong Zhou | Leming Cheng | Qinhui Wang | Zhongyang Luo | Kefa Cen

In large-scale circulating fluidized bed (CFB) boilers, it is common to use multiple cyclones in parallel for the capture of solids, assuming that gas-solid flow to be the same in the cyclones. This article presents a study investigating gas-solid flow through six parallel cyclones in a CFB cold test rig. The six cyclones were located asymmetrically on the left and right walls of the riser. Solid volume fraction and particle velocity profiles at the riser outlets and in the horizontal ducts were measured using a fiber optical probe. Cyclone pressure drop and solid circulating rate were measured for each individual cyclone. Measurements showed good agreement as to the non-uniform distribution of the gas-solid flow, which occurred mainly across the three cyclones on one side: the middle cyclones on both sides had higher particle velocities. Conversely, the solid volume fractions, solid fluxes and solid circulating rates of the middle cyclones were lower than those of the other four cyclones. The apparent reason for the flow non-uniformity among the cyclones is the significant flow non-uniformity at the riser outlets. Under typical operating conditions, the solid volume fractions at the riser outlets had a deviation of up to 26% whereas the solid circulating rates at the stand pipes, 7%. These results are consistent with most other studies in the literature. © 2012 Chinese Society of Particuology and Institute of Process Engineering, Chinese Academy of Sciences. Published by Elsevier B.V. All rights reserved.

Solvent-less synthesis of zinc oxide nanostructures from Zn(salen) as precursor and their optical

properties ↗

Volume 10, Issue 6, December 2012, Pages 759-764

Ali Kazemi Babaheydari | Masoud Salavati-Niasari | Afsaneh Khansari

ZnO nanoparticles, 10-20 nm in size, were synthesized by heat treatment in air at 500 °C for 5 h., using [N,N′-bis(salicylaldehydo) ethylene diamine]zinc(II), i.e., Zn(salen), as precursor, which was obtained by a solvent-free solid-solid reaction. Heat-treated products were characterized by X-ray diffraction, Fourier transform infrared spectroscopy, scanning electron microscopy, and transmission electron microscopy. Room temperature photoluminescence spectra of ZnO nanostructures are dominated by green emission attributed to oxygen vacancy related donor-acceptor transition. © 2012 Chinese Society of Particuology and Institute of Process Engineering, Chinese Academy of Sciences.

Recent status of fluidized bed technologies for producing iron input materials for steelmaking ↗

Volume 9, Issue 1, February 2011, Pages 14-23

Johannes Leopold Schenk

Today steel is produced by two steelmaking processes, the basic oxygen furnace and the electric arc furnace. Three types of iron input materials for both processes are liquid hot metal or in solidified form as pig iron, direct reduced iron (DRI) and hot briquetted iron (HBI) as well as steel scrap. Hot metal, pig iron, DRI and HBI are virgin iron materials, which have to be produced from iron ore by the so-called ironmaking technologies. New ironmaking processes based on fluidized bed technology have been developed in the last two decades. The main advantage of these technologies is that fine ore can be directly used in the processes and prior treatment such as sintering or pelletizing can be avoided which is required for the established processes. Theoretical

aspects for reduction of fine iron oxides in a fluidized bed reactor system will be explained. The fluidized bed reducing technologies utilized in the most advanced new ironmaking processes for direct use of fine ore, FINMET®, Circored®, FINEX® and HIsmelt® will be compared. © 2010 Chinese Society of Particuology and Institute of Process Engineering, Chinese Academy of Sciences.

Chemical characteristics of PM2.5 during haze episodes in the urban of Fuzhou, China ↗

Volume 11, Issue 3, June 2013, Pages 264-272

Fuwang Zhang | Lingling Xu | Jinsheng Chen | Xiaoqiu Chen | Zhenchuan Niu | Tong Lei | Chunming Li | Jinping Zhao

Atmospheric fine particles (PM2.5) were collected in this study with middle volume samplers in Fuzhou, China, during both normal days and haze days in summer (September 2007) and winter (January 2008). The concentrations, distributions, and sources of polycyclic aromatic hydrocarbons (PAHs), organic carbon (OC), elemental carbon (EC), and water soluble inorganic ions (WSIIs) were determinated. The results showed that the concentrations of PM 2.5, PAHs, OC, EC, and WSIIs were in the orders of haze > normal and winter > summer. The dominant PAHs of PM2.5 in Fuzhou were Fluo, Pyr, Chr, BbF, BkF, BaP, BghiP, and IcdP, which represented about 80.0% of the total PAHs during different sampling periods. The BaPeq concentrations of ∑PAHs were 0.78, 0.99, 1.22, and 2.43 ng/m3 in summer normal, summer haze, winter normal, and winter haze, respectively. Secondary pollutants (SO4 2-, NO3 -, NH4 +, and OC) were the major chemical compositions of PM2.5, accounting for 69.0%, 55.1%, 63.4%, and 64.9% of PM2.5 mass in summer normal, summer haze, winter normal, and winter haze, respectively. Correspondingly, secondary organic carbon (SOC) in Fuzhou accounted for 20.1%, 48.6%, 24.5%, and 50.5% of OC. The average values of nitrogen oxidation ratio (NOR) and sulfur oxidation

ratio (SOR) were higher in haze days (0.08 and 0.27) than in normal days (0.05 and 0.22). Higher OC/EC ratios were also found in haze days (5.0) than in normal days (3.3). Correlation analysis demonstrated that visibility had positive correlations with wind speed, and negative correlations with relative humidity and major air pollutants. Overall, the enrichments of PM2.5, OC, EC, SO4 2-, and NO3 - promoted haze formation. Furthermore, the diagnostic ratios of IcdP/(IcdP + BghiP), IcdP/BghiP, OC/EC, and NO3 -/SO 4 2- indicated that vehicle exhaust and coal consumption were the main sources of pollutants in Fuzhou.

© 2012 Published by Elsevier B.V.

Pore-structure-mediated hierarchical SAPO-34: Facile synthesis, tunable nanostructure, and catalysis applications for the conversion of dimethyl ether into olefins

Volume 11, Issue 4, August 2013, Pages 468-474

Yu Cui | Qiang Zhang | Jie He | Yao Wang | Fei Wei

Hierarchical cross-like SAPO-34 catalysts with different pore size distributions were obtained via hydrothermal synthesis with polyethylene glycol (PEG) as the mesopore-generating agent. The hierarchical SAPO-34 molecular sieves were characterized using X-ray diffraction, scanning electron microscopy, N2 adsorption-desorption, thermogravimetric analysis, and temperature-programmed NH3 desorption. The cross-like SAPO-34 catalysts exhibited enriched multi-porosity, and the sizes of their mesopores ranged from 10 to 50 nm. Both the mesoporous structures and morphologies of the hierarchical SAPO-34 could be further tuned through adjustments of the amount of PEG used. The as-obtained SAPO-34 showed dramatic catalytic performance in the conversion of dimethyl ether into olefins. A maximum selectivity of olefins of 96% was achieved, which was

attributed to the rapid transport of the reactants and products in zeolitic micropores through mesopores. © 2013 Chinese Society of Particuology and Institute of Process Engineering, Chinese Academy of Sciences. Published by Elsevier B.V. All rights reserved.

Preparation and activity evaluation of NiMoB/γ-Al2O 3 catalyst by liquid-phase furfural hydrogenation

Volume 9, Issue 1, February 2011, Pages 69-74

Shuqin Wei | Hongyou Cui | Jinghua Wang | Shuping Zhuo | Weiming Yi | Lihong Wang | Zhihe Li

Amorphous MoNiB/γ-Al2O3 alloy catalysts were prepared by reducing NiCl2·6H2O and (NH 4)6Mo7O24·4H2O supported on γ-Al2O3 with NaBH4 as reducing agent. Using liquid-phase hydrogenation of furfural (FFR) as a probe reaction, the activity of MoNiB/γ-Al2O3 was examined. Compared to NiB and NiMoB, NiMoB/γ-Al2O3 exhibited excellent activity and selectivity towards furfuryl alcohol (FFA). After reaction for 3.0 h at 80 °C and 5.0 MPa in methanol, FFR conversion reached 99% with FFA yield of 91%. The effects of doping amount of Mo and calcination temperature before NaBH4 reduction on hydrogenation activity were also investigated. The optimum Mo/Ni atom ratio and calcination temperature were found to be 1:7 and 300 °C, respectively. XRD patterns and SEM images indicated that NiMoB over the surface of γ-Al2O 3 was amorphous and highly dispersed, which was responsible for the high thermal stability of the title catalyst. © 2010 Chinese Society of Particuology and Institute of Process Engineering, Chinese Academy of Sciences.

Parallel computing of discrete element method on multi-core processors

Volume 9, Issue 4, August 2011, Pages 398-405

Yusuke Shigeto | Mikio Sakai

This paper describes parallel simulation techniques for the discrete element method (DEM) on multi-core processors. Recently, multi-core CPU and GPU processors have attracted much attention in accelerating computer simulations in various fields. We propose a new algorithm for multi-thread parallel computation of DEM, which makes effective use of the available memory and accelerates the computation. This study shows that memory usage is drastically reduced by using this algorithm. To show the practical use of DEM in industry, a large-scale powder system is simulated with a complicated drive unit. We compared the performance of the simulation between the latest GPU and CPU processors with optimized programs for each processor. The results show that the difference in performance is not substantial when using either GPUs or CPUs with a multi-thread parallel algorithm. In addition, DEM algorithm is shown to have high scalability in a multi-thread parallel computation on a CPU. © 2011 Chinese Society of Particuology and Institute of Process Engineering, Chinese Academy of Sciences. All rights reserved.

Chemical characteristics of PM2.5 during dust storms and air pollution events in Chengdu, China ↗

Volume 11, Issue 1, February 2013, Pages 70-77

Qiyuan Wang | Junji Cao | Zhenxing Shen | Jun Tao | Shun Xiao | Lei Luo | Qingyang He | Xinying Tang

Daily fine particulate (PM2.5) samples were collected in Chengdu from April 2009 to February 2010 to investigate their chemical profiles during dust storms (DSs) and several types of pollution events, including haze (HDs), biomass burning (BBs), and fireworks displays (FDs). The highest PM 2.5 mass concentrations were found during DSs (283.3 μg/m 3), followed by FDs (212.7 μg/m3), HDs (187.3 μg/m3), and

BBs (130.1 μg/m3). The concentrations of most elements were elevated during DSs and pollution events, except for BBs. Secondary inorganic ions (NO3 -, SO4 2-, and NH4 +) were enriched during HDs, while PM2.5 from BBs showed high K+ but low SO4 2-. FDs caused increases in K+ and enrichment in SO 4 2-. Ca2+ was abundant in DS samples. Ion-balance calculations indicated that PM2.5 from HDs and FDs was more acidic than on normal days, but DS and BB particles were alkaline. The highest organic carbon (OC) concentration was 26.1 μg/m3 during FDs, followed by BBs (23.6 μg/m3), HDs (19.6 μg/m3), and DSs (18.8 μg/m3). In contrast, elemental carbon (EC) concentration was more abundant during HDs (10.6 μg/m3) and FDs (9.5 μg/m3) than during BBs (6.2 μg/m3) and DSs (6.0 μg/m3). The highest OC/EC ratios were obtained during BBs, with the lowest during HDs. SO4 2-/K+ and TCA/SO 4 2- ratios proved to be effective indicators for differentiating pollution events. Mass balance showed that organic matter, SO4 2-, and NO3 - were the dominant chemical components during pollution events, while soil dust was dominant during DSs. © 2012 2012 Chinese Society of Particuology and Institute of Process Engineering, Chinese Academy of Sciences. Published by Elsevier B.V. All rights reserved.